Signal Processing 157 (2019) 280–287

Contents lists available at ScienceDirect

Signal Processing

journal homepage: www.elsevier.com/locate/sigpro

Compressed sensing for image reconstruction via back-off and rectification of greedy algorithm

Qingyong Deng[a], Hongqing Zeng[a], Jian Zhang[b], Shujuan Tian[a,*], Jiasheng Cao[a], Zhetao Li[a], Anfeng Liu[c]

[a] College of Information Engineering, Xiangtan University, Xiangtan 411105, China
[b] School of Science & Technology, Zhejiang International Studies University, Hangzhou 3100, China
[c] School of Information Science and Engineering, Central South University, ChangSha 410083, China

ARTICLE INFO

Article history:
Received 13 July 2017
Revised 14 December 2017
Accepted 10 December 2018
Available online 11 December 2018

Keywords:
Image reconstruction
Compressive sensing
Sparse signal reconstruction
Back-off and rectification
Greedy pursuit

ABSTRACT

Image reconstruction is an important research topic in the field of multimedia processing. It aims to represent a high-resolution image with highly compressed features that can be used to reconstruct the original image as well as possible, and has been widely used for image storage and transmission. Compressed Sensing (CS) is a commonly used approach for image reconstruction; however, CS currently lacks an efficient and accurate solving algorithm. To this end, we present an iterative greedy reconstruction algorithm for Compressed Sensing called back-off and rectification of greedy pursuit (BRGP). The most significant feature of the BRGP algorithm is that it uses a back-off and rectification mechanism to select the atoms and then obtains the final support set. Specifically, an intersection of support sets estimated by the Orthogonal Matching Pursuit (OMP) and Subspace Pursuit (SP) algorithms is first set as the initial candidate support, and then a back-off and rectification mechanism is used to expand and rectify it. Experimental results show that the algorithm significantly outperforms conventional techniques for one-dimensional or two-dimensional compressible signals.

1. Introduction

With the development of the Internet of Things (IoT) [1, 2], software defined networks (SDN) [3, 4], and cloud computing [5–7], recent years have witnessed a boom of images and videos generated by popularly used digital cameras. The vast quantities of images and videos brings about a series of problems for current Internet applications, such as image quality assessment [8], image classification [9,10], image defect inspection [11], image recovery [12,13] and feature selection [14]. The most obvious problem is that these media data require a lot of storage space [15, 16], therefore methods to transform these images and videos into more compressed data representations and achieve perfect data reconstruction from those representations have become a hot research topic in the field of multimedia processing.

A typical group of approaches to image compression is based on the Shannon-Nyquist sampling theorem, which indicates that the perfect image reconstruction may require the sampling rate to be two times higher than the original sampling rate of the image [17, 18]. Thus, Shannon's theory places an obstacle in the way of further improvements in the image compression rate and reconstruction algorithms.

As commonly noted, the data dimension of an image is very high, but not all of the information in an image is meaningful in understanding the semantics of the image. Therefore, an image usually contains much redundant information, and it is reasonable to assume the most useful information for depicting the semantics of the image is sparse [19–21]. Enlighted by the sparsity assumption, Candès et al. proposed the Compressed Sensing (CS) method [17,18], which has attracted much attention as a method to acquire, measure and reconstruct sparse signals [22–26]. Owing to the sparsity assumption, it allows us to sample signals at a rate which is significantly below the Shannon-Nyquist rate and reconstruct signals with high probability from very few measurements.

Generally, image reconstruction algorithms based on the CS method can be divided into three groups, i.e., convex optimization algorithms, combinatorial algorithms and greedy algorithms. Convex optimization replaces the l_0 norm minimization of the original CS problem with l_1 norm minimization, so that the problem can be made convex and solved using existing methods. In many cases,

* Corresponding author.
E-mail addresses: dengqingyong@xtu.edu.cn (Q. Deng), zenghongqing-sf@qq.com (H. Zeng), jeyzhang@outlook.com (J. Zhang), sjtianwork@xtu.edu.cn (S. Tian), 986766214@qq.com (J. Cao), liztchina@gmail.com (Z. Li), afengliu@csu.edu.cn (A. Liu).

https://doi.org/10.1016/j.sigpro.2018.12.007
0165-1684/

the solution is very similar to that of the original problem, but there still exists some deviation from the true solution of the original problem. Combinatorial algorithms acquire highly structured samples of the signal that support rapid reconstruction via group testing. This group of methods includes Fourier sampling [27,28], chaining pursuit [29], HHS pursuit [30] and so on. Combinatorial algorithms are less complex than convex relaxation methods, but at the cost of higher sample/equation requirements. The low computational costs of combinatorial algorithms stem from the fact that these approaches are based on binary sparse projection matrices, and this is sometimes not coincident with the real conditions. Greedy algorithms are iterative methods for approximating a signal from compressed samples. In each iteration process, they use a greedy rule to identify the position of nonzero elements in a sparse signal. We are particularly interested in greedy algorithms because they try to approximate the solution of l_0 minimization problems directly and have fast reconstruction speeds and low reconstruction complexity. There are two commonly used greedy algorithms: single atom and multiple atom algorithms. The multiple atom algorithm is an enhanced version of the single atom algorithm. However, current algorithms still cannot select atoms adaptively and delete wrong atoms effectively, which may influence the accuracy of image reconstruction.

To this end, we propose an algorithm referred to as back-off and rectification of greedy pursuit (BRGP). Firstly, an intersection of support sets estimated by the Orthogonal Matching Pursuit (OMP) and the Subspace Pursuit (SP) algorithm is set as an initial candidate support sets. Secondly, a back-off and rectification mechanism is then used to expand and rectify it. Finally, the target signal x can be estimated. The advantages of the proposed algorithm are twofold:

1. It selects atoms adaptively and deletes incorrect atoms effectively while computing the sparse representation of the signals, and this leads to a more accurate support set so that the accuracy of signal reconstruction is guaranteed.
2. It aims to directly optimize the l_0 norm minimization problem. Without l_1 norm relaxation, the solution could be much closer to that of the original problem.

The remainder of this paper is organized as follows. Section 2 summarizes works related to reconstruction algorithms in CS. Section 3 introduces the process of back-off and rectification of greedy pursuit algorithm. Section 4 provides analysis of the BRGP algorithm. Section 5 makes a comparison of our work with related algorithms using simulations. Section 6 shows the conclusion.

2. Related work

There have been some previous strategies that are relevant to the strategy of context-aware sensing and collection of data. We categorize these studies as following:

Compressed Sensing (CS) is designed to reconstruct a sparse signal $\boldsymbol{x}$ satisfying $\|x\|_0 = K \ll N \ \ (x \in \mathbb{R}^{N\times 1})$, and the objective function in the standard sensing modality can be represented as

$$b = \Phi x + w, \tag{1}$$

where $b \in \mathbb{R}^{M\times 1}$ is the acquired measurement vector, $\Phi \in \mathbb{R}^{M\times N}$ is a sensing matrix, and $\boldsymbol{w}$ is a noise vector.

The reconstruction of an original sparse signal x is well-formulated as an l_0-minimization problem. The sparsest solution of an underdetermined system is given by

$$\min_x \|x\|_0, \quad \text{subject to } \Phi x = b. \tag{2}$$

Since l_0-minimization is NP-hard, early works mainly focused on transforming the l_0-minimization problem into an l_1-minimization problem.

Many approaches have been proposed for reconstructing signals and images using compressed sensing theory [31]. Commonly used reconstruction algorithms are based on convex optimization algorithms, combinatorial algorithms, and greedy algorithms. The convex optimization methods attempt to reconstruct signals by solving the mathematical program

$$\min \|b\|_1 or \|b\|_p, \ \text{subject to } \|\Phi b - u\|_2 \le \varepsilon, \tag{3}$$

where $\|\cdot\|_p$ denotes the pth norm, and we assume the norm of the noise vector $\|e\|_2 \le \varepsilon$. The linear programming (LP) algorithm can solve (3) and is known as Basis Pursuit (BP) [32]. Unfortunately, the complexity of the LP is cubic (i.e., O(N^3)), which makes it infeasible for practical and large-scale applications.

The low computational costs of combinatorial algorithms stem from the fact that these approaches are based on binary sparse projection matrices. Gilbert et al. [29] indicates that a typical combinatorial decoder for CS is in fact a simple recursive l_1-minimizer in the case of a binary projection matrix. However, the authors did not mention how to replace the non-zero entries of the projection matrix with random variables, which is the more common case in many real applications.

Another group of approaches to sparse signal reconstruction is based on the idea of iterative greedy pursuit, which tries to approximate the solution of l_0-minimization problem directly. Greedy algorithms are iterative methods for approximating a signal from compressed samples. In each iteration process, they use a greedy rule to identify the position of nonzero elements of sparse signal. There are two types of algorithms, classified according to the way the atoms are added: single atom and multiple atom algorithms.

Some representative single atom algorithms are Orthogonal Match Pursuit (OMP) [33], Look Ahead Orthogonal Match Pursuit (LAOMP) [34], and Multipath Matching Pursuit (MMP) [35]. The major advantages of OMP lie in its speed and ease of implementation. The major advantages of the LAOMP are the same as those of the OMP. However, once an atom is added into the support set of those algorithms, it cannot be deleted. The performance of MMP algorithms is good, but the computational complexity of MMP is very high.

In many applications, single atom algorithms update the support set permanently and thus cannot make good performance. Therefore, some researchers have developed pursuit methods that work better in performance and yield essentially optimal theoretical guarantees, called multiple atom algorithms. Multiple atom algorithms update the support set by adding several atoms in each iteration, such as Stagewise Orthogonal Matching Pursuit (StOMP) [36], Subspace Pursuit (SP) [37], Compressive Sampling Matching Pursuit (CoSaMP) [38], Modified version of CoSaMP (Modified-CoSaMP) [39], Multipath Subspace pursuit (MSP) [40], and Fusion of Algorithms for Compressed Sensing (FACS) [41], etc. The advantages of these algorithms are their speed and low computational demand. However, StOMP cannot delete atoms that have been added into the support set. CoSaMP chooses $2K$ atoms in an iteration, which weakens the performance of least-squares and hence causes deterioration in the sparse signal recovery performance. SP is similar to CoSaMP. Modified-CoSaMP adaptively chooses the dimension of the search space in each iteration, using a threshold based approach. Neither CoSaMP nor Modified-CoSaMP can guarantee that the columns of selected measurement matrix are uncorrelated. MSP does not perform well in noisy scenarios. FACS uses a fusion framework, in which multiple sparse signal recovery algorithms are employed and their estimates fused to get a better estimate, but the FACS still cannot select atoms adaptively and the search space is smaller than for SP. All in all, greedy pursuit al-

gorithms have the advantages of low computational demand and simple geometric interpretation, therefore they have been widely used in medical image processing and in wireless sensor networks [42].

3. Back-off and rectification greedy pursuit

In Sections 3 and 4, we will introduce a novel back-off and rectification greedy pursuit (BRGP) method for solving the l_0-minimization problem in detail. The following are the meaning of the mathematical notations used in Sections 3 and 4: $\|\cdot\|_p$ denotes the p^{th} norm. Φ_Γ denotes the column sub-matrix of which the indices of the columns are the elements of the set Γ. x_Γ denotes the sub-vector formed by those elements whose indices are listed in the set Γ. $\lfloor\cdot\rfloor$ denotes the floor function.

3.1. The BRGP algorithm

An intersection of the support sets estimated by different types of algorithms is probably a subset of the target support set. Based on this concern, we develop the back-off and rectification greedy pursuit (BRGP) method. In order to speed up the run time of the algorithm, the OMP and SP algorithms are used to obtain the intersection of the support set as the initial candidate support set λ, and the initial residual r can be calculated. We use the following iteration scheme:

Step 1: Determine whether iteration operates back-off

For a new residual r_{new}, if $\|r - r_{new}\|_2$ is smaller than a certain threshold ε (the range of ε can be known from Section 4), use $F := \{j : |\Phi_j^T r| > u \times \max_{j=1:N} |\Phi_j^T r|\}$ $(\mu \in [0, 1])$ to expand the candidate support set λ, otherwise return to the last iteration and then add an atom to λ by using $F := \arg\max_{j=1,2,\cdots,d} \langle r, \Phi_j \rangle$, where $\langle , \rangle$ represents the inner product of r and Φ_j. The iteration will not stop until the length of λ is K, then the residual and the support set λ of each stage are saved.

Step 2: Rectify the support set

At the first iteration, the length of the search space is $T = K$, and the decreasing subspace pursuit method expands the selected support set with indices of the T largest magnitude entries of $\Phi^T r$. The size of the extended support set S^k *is* $T + K$, and then the orthogonal projection coefficients of b onto Φ_{S^k} are computed, and the estimated support S^k is obtained by pruning S^k to contain only K indices corresponding to the largest elements of $\Phi_{S^k}^\dagger b$. In later iterations of the process, the length of the search space is reduced by using $T = \alpha * T$ $(0 < \alpha < 1)$, and the execution is the same as for the first iteration operation. The iteration process is stopped when T=0. Lastly, the final support set $S = \lambda$ and the final estimated signal x are obtained.

The proposed BRGP algorithm is summarized as Algorithm 1, and the sub-processes of rectifying the support set are summarized as Algorithm 2.

3.2. Interpretation of back-off and rectification

The term back-off and rectification comes from the processes of the algorithm. The process of determining whether back-off operates in each iteration is based on comparing the current iteration with the last iteration (i.e. there is a transition stage). Suppose that two adjacent iteration residuals are r and r_{new}, respectively. If the value of $\|r - r_{new}\|_2$ is greater than a certain threshold, the current iteration should operate back-off (return to the last iteration) and restart the process of choosing an atom, otherwise atoms should be added directly. When the value of $\|r - r_{new}\|_2$ is too large (above the threshold), it means that incorrect atoms have likely been added into the support set, and back-off thus operates in order to improve the possibility of selecting correct atoms.

The process of rectification is based on the use of a decreasing subspace pursuit method, similar to the SP algorithm, to rectify the candidate support set. According to Gilbert and Strauss [28], there are 2 K indices in candidate support set λ, among which at least K of them do not belong to the target support set T in the iteration process, and a good estimation of the support set can be obtained via the largest projection coefficients. Similarly, if there are $K + L$ indices in the set λ, the remaining steps are the same and a good support set can be also obtained in this iteration process. From Lemma 2 of Section 4, during the process of selecting atoms, if we assume that the candidate support set $\lambda = \{\lambda_1, \lambda_2, \cdots, \lambda_t\}$ is selected, we have $\Phi_\lambda^* b_t = 0$, which guarantees orthogonality between the residue b_t and the final support set $S = \lambda$. Thus, we know that the approximate solution obtained from the BRGP is optimal in the sense of approximating K nonzero elements in the original signal when the final support set is obtained.

The main contribution of the BRGP reconstruction algorithm is that it creates a back-off and rectification mechanism that realizes trade-offs between computational complexity and reconstruction performance.

Algorithm 1 Back-off and rectification of greedy pursuit.

Inputs: Sensing matrix Φ, measurement vector b, sparsity level K, transition stage parameter ε, u, a pre-set constant in [0, 1], and the backtracking subspace parameter T, α.

$J_{OMP} = OMP(\Phi, b, K)$; // OMP support set

$J_{SP} = SP(\Phi, b, K)$; // SP support set

initial candidate support set $\lambda = J_{OMP} \cap J_{SP}$;

Initialization:

$x_\lambda := \Phi_\lambda^\dagger b, r := b - \Phi x_\lambda$;

$F := \{j : |\Phi_j^T r| > u \times \max_{j=1:N} |\Phi_j^T r|\}, x_\lambda = \Phi_\lambda^\dagger b, r_{new} := b - \Phi x_\lambda$;

save the residuals and the candidate support set of each stage;

update the latest candidate support set and the final support set $S = \emptyset$, $m := \|\lambda\|_0$;

While $m < K$ **Do**

  IF $\|r - r_{new}\|_2 \le \varepsilon$ **then**

    $F := \{j : |\Phi_j^T r| > u \times \max_{j=1:N} |\Phi_j^T r|\}$;

    save the set λ and update λ with $\lambda = \lambda \cup F$;

  Else

    return to the last iteration;

    $F := \arg\max_{j=1,2,\cdots,d} \langle r, \Phi_j \rangle$;

    save the set λ and update λ with $\lambda = \lambda \cup F$;

  End if

  $m := \|\lambda\|_0$; $S := \lambda$; $x_S := \Phi_S^\dagger b$; $r_{new} := b - \Phi x_S$;

  save the residuals and the support set of each stage;

End while

$[x, S] = \text{Rectify}Support(\Phi, T, K, S, b, r_{new}, \alpha)$;

Output: x (estimated signal), S(estimated support set);

Algorithm 2 Rectify support function.

Inputs: Sensing Matrix Φ, measurement vector b, sparsity level K, the support set S, the backtrack subspace parameter T, α and the initial residual r_{new};

Initialization: r_{new};

While $T! = 0$ do

  $\Lambda :=$ {indices of T highest amplitude components of $\Phi^T r_{new}$};

  $S := S \cup \Lambda$; $\widehat{x} := A_S^\dagger b$;

  $S :=$ {indices corresponding to the K largest magnitude components of $\widehat{x}$};

  $x := \Phi_S^\dagger y$; $r_{new} := b - \Phi x$; $T := \alpha * T$;

End while

Output: x (estimated signal), S(estimated support set);

4. Theoretical analysis

In this section, we first introduce some theorems or lemmas that are useful for robustness analysis, and then provide robustness analysis for the back-off and rectification algorithm. Finally, the computational complexity of the BRGP is provided.

4.1. Incorporation of prior information

We first briefly review some well-known theorems that are useful for robustness analysis.

A widely-used condition of Φ ensuring the exact reconstruction of x is called Restricted Isometry Property (RIP). A sensing matrix Φ should satisfy the RIP of order K if there is a constant $\delta \in (0, 1)$ such that

$$(1-\delta)\|x\|_2^2 \le \|\Phi x\|_2^2 \le (1+\delta)\|x\|_2^2. \tag{4}$$

For any K-sparse vector$x$, the minimum of all constants $\delta(\Phi)$ satisfying (3) is called the restricted isometry constant δ_K.

Lemma 1. (Consequence of RIP)

(1) (Monotonicity of δ_K) For any two integers$K \le K'$,

$$\delta_K \le \delta_{K'}. \tag{5}$$

(2) (Near-orthogonality of columns) Let$I,J \subset \{1, \cdots, N\}$ be two disjoint sets, $I \cap J = \emptyset$. Suppose $\delta_{|I|+|J|} < 1$for arbitrary vectors $a \in \mathbb{R}^{|I|}$ and $b \in \mathbb{R}^{|J|}$,

$$\left|\left\langle \Phi_I a, \Phi_J b \right\rangle\right| \le \delta_{|I|+|J|}\|a\|_2\|b\|_2, \tag{6}$$

and

$$\left\|\Phi_I^T \Phi_J b\right\|_2 \le \delta_{|I|+|J|}\|b\|_2. \tag{7}$$

Lemma 2. Let measurement vector $b \in \mathbb{R}^m$ and sensing matrix $\Phi_I \in \mathbb{R}^{m\times|I|}$. Suppose $\Phi_I^T\Phi_I$ is invertible, the projection of $b$onto span Φ_I is defined as

$$b_p = proj(b, \Phi_I) := \Phi_I \Phi_I^{\dagger} b, \tag{8}$$

where

$$\Phi_I^{\dagger} := \left(\Phi_I^T \Phi_I\right)^{-1} \Phi_I^T. \tag{9}$$

$\Phi_I^{\dagger}$ denotes the pseudo-inverse of the matrixΦ_I, and T stands for matrix transposition.

The residual vector of the projection equals

$$b_r = reside(b, \Phi_I) := b - b_p. \tag{10}$$

(Orthogonality of the residual) For an arbitrary vector $b \in \mathbb{R}^m$ and a sampling matrix $\Phi_I \in \mathbb{R}^{m\times N}$ of full column rank, let $b_r = resid(b, \Phi_I)$, then

$$\Phi_I^T b_r = \Phi_I^T (b - \Phi_I(\Phi_I^T\Phi_I)^{-1}\Phi_I^T b) = 0. \tag{11}$$

Lemma 3. Let the columns of Φ be in general position. Let I_S denote the support set of $\widehat{x}_s$. Suppose the support set I_0 of x_0 is a subset of I_S. In addition, supposing that $\#I_S \le n$. Then we have perfect recovery:

$$\widehat{x}_s = x_0. \tag{12}$$

4.2. Robustness analysis of the back-off and rectification algorithm

The robustness of the back-off and rectification algorithm depends on the processes of the transition stage and the decreasing subspace pursuit. In the transition stage, robustness can be analyzed as follows:

In the process of determining whether to back-off, the candidate support set is expanded. From Lemma 1, the condition of adaptive selection of an atom can be formulated as follows:

$$\begin{aligned} &\|r - r_{new}\|_2 = \|(b - \Phi_\lambda x - (b - \Phi_{\lambda\cup F}x)\|_2 \\ &= \|(\Phi_{\lambda\cup F}x - \Phi_\lambda x)\|_2 \\ &= \left\|\Phi_F \Phi_C^T b_C\right\|_2 \\ &\le \delta_{|F|+|C|}\|b_C\|_2 \le \delta_K\|b\|_2 = \varepsilon < \|b\|_2, \end{aligned} \tag{13}$$

where C is the target support set, and λ is the estimate support set.

If the condition$\|r - r_{new}\|_2 > \varepsilon$ is satisfied, it is deemed that some incorrect atoms have been added to the candidate support set λ in this iteration. Therefore, the algorithm should return to the last iteration and restart the selection of a single atom, which guarantees that a correct atom is added to the support set. We can recover x from Lemma 3 in [27]. Lemmas 1 and 2 are obtained in [28].

The iterative number of the decreasing subspace method is $n = \lfloor \log K \rfloor$. A feature of the decreasing subspace pursuit process is that the length of search subspace L is continuously halved until $\lfloor L \rfloor = 0$ through n iterations.

Lemma 4. Let $x \in \mathbb{R}^N$ be a K-sparse vector, $\|x\|_0 \le K$; the support set is C and let $b = \Phi x$ be a measurement for which $\Phi \in \mathbb{R}^{m\times N}$ satisfies the RIP with parameter δ_K. For an arbitrary $\lambda \subset \{1, \cdots, N\}$ such that $|\lambda| \le K$, define $\hat{x}$ as

$$\widehat{x}_\lambda = \Phi_\lambda^{\dagger} b, \tag{14}$$

and

$$\widehat{x}_{\{1,\cdots,N\}-\lambda} = 0, \tag{15}$$

$$\|x - \widehat{x}\|_2 \le \frac{1}{1-\delta_{3K}}\|x_{C-\lambda}\|_2. \tag{16}$$

Since the length of subspace $L \le K$, supposing that upper bound of the sampling matrix in the decreasing subspace method satisfies $\delta_K \le \delta_\tau \le \delta_{3K}$ according to Lemma 1, then

$$\|x - \widehat{x}\|_2 \le \frac{1}{1-\delta_\tau}\|x_{C-\lambda}\|_2 \le \frac{1}{1-\delta_{3K}}\|x_{C-\lambda}\|_2. \tag{17}$$

During the process, the estimated support set λ, comprising indices corresponding to the K largest magnitude components of $\widehat{x}$, gradually approaches C, which makes $\|x - \widehat{x}\|_2 \to 0$ and realizes the robustness effect. Lemma 3 is related to a modification of Theorem 3 in [28].

4.3. Computational complexity analysis of the BRGP

The BRGP algorithm includes three sections: initialization, determination of whether or not to back-off, and decreasing subspace pursuit. The complexity of the initialization process depends on the running of the OMP and SP algorithms. We know that the complexity of both the OMP and the SP is $O(MNK)$, so the complexity of the initialization process is $O(MNK)$. The complexity of determining whether or not to back-off includes the complexity of adding atoms directly and that of operating back-off to add atoms, which is $\{j : |\Phi_j^T r| > u \times \max_{j=1:N} |\Phi_j^T r|\}$ and $\arg\max_{j=1,2,\cdots,d} \langle r, \Phi_j \rangle$ are around $O(NM)$,$O(MN)$ respectively, so the complexity of the loop process is upper bounded by O(KMN). The complexity of the SP is O(KMN) and the number of selecting atoms is K in each iteration. However, in the decreasing subspace method the number of selecting atoms is reduced in each iteration, and the complexity of the decreasing subspace method is thus bounded by $O(MN)$. Therefore, the total computational complexity of the BRGP is $O(KMN)$.

5. Simulation and results

In this section, we report some experimental results for sparse signal reconstruction using our proposed BRGP method and several state-of-the-art methods: OMP, StOMP, Modified-CoSaMP and FACS (Fusing OMP with SP). We also present evaluation and analysis of these experimental results. The experiments cover both one-dimensional signals and two-dimensional images, and the evaluation metrics include reconstruction accuracies, run times, Average Support Cardinality Errors (ASCE) and Peak Signal to Noise Ratios (PSNR).

5.1. Reconstruction of sparse signals in which the non-zero values obey N(0, 1)

In this experiment, the signal is a randomly generated Gaussian sparse signal with a length of $N = 256$. The partial FFT sensing operator is used, with a fixed number of measurements $M = 128$. We aim to investigate the frequency of exact reconstruction and the mean reconstruction time vs. the signal sparsity K for a given M, among 1000 repeated implementations. Different sparsity levels are chosen from $K = 1$ to $K = 64$, and for each K, 1000 experiments are conducted to calculate the frequency of exact reconstruction and the mean reconstructive time for each of the algorithms.

Fig. 1(a) shows that the BRGP performs better than OMP, StOMP, Modified-CoSaMP and FACS when the nonzero entries of the sparse signal are drawn from $N(0, 1)$ and the remaining coefficients of $\boldsymbol{x}$ are set to 0. We can see that the frequency of exact reconstruction is 1 at low sparsity levels, but the reconstructive signal is not accurate when the sparsity level above a certain value. More measurements are needed to achieve a better reconstructed signal. Furthermore, the results in Fig. 1(a) show that OMP, StOMP, Modified-CoSaMP and FACS can accurately reconstruct the signal at sparsity levels of 21, 38, 37, and 45 respectively, while BRGP extends the sparsity level to 47. Fig. 1-(b) shows that the mean reconstruction time for BRGP, OMP, StOMP, and FACS algorithms at $1 \le K \le 64$. The mean reconstructive time of the BRGP is only shorter than that for the StOMP when $1 \le K \le 43$, and increases rapidly as the sparsity level increases.

In Fig. 1(a), the performance of OMP, StOMP, CoSaMP and FACS become poor when the sparsity level K is high. Because the OMP and the StOMP algorithms cannot delete incorrect atoms, the modified-CoSaMP method cannot guarantee that L (set by the modified-CoSaMP) columns of the selected measurement matrix are uncorrelated in each iteration, and the FACS selects atoms from the union support set of the OMP and the SP. However, the BRGP algorithm can operate back-off when incorrect atoms are selected. Furthermore, BRGP uses a decreasing subspace pursuit method to rectify the support set. Thus, when the sparsity level K is higher, the reconstructive accuracy of BRGP is better than the other methods. In Fig. 1(b), from Section 3, the computational complexity of BRGP is the same as for OMP, StOMP, and FACS, which for all of them is $O(MNK)$. However, the iteration number for BRGP is only smaller than for StOMP, which makes the run time for BRGP only shorter than for StOMP when the sparsity level below 43.

5.2. Indirectly reconstructed weighted 0–1 sparse signal

We use the same setup as for experiment 1. For each sparsity level K, we generate a signal$x$, in which the nonzero coefficients are set to 1 and then x is weighted by $t = [1/N^2, 2^2/N^2, \cdots, N^2/N^2]$. Our aim is to investigate the frequency of exact reconstruction and the mean reconstructive time vs. the signal sparsity level K for a given M. Different sparsity levels are chosen from 1 to 64, and for each K, 1000 simulations were conducted to calculate the frequency of exact reconstruction and the mean reconstructive time for the different algorithms.

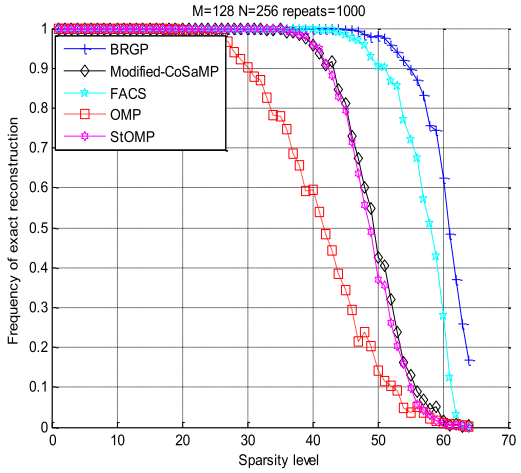

(a) Frequency of exact reconstruction

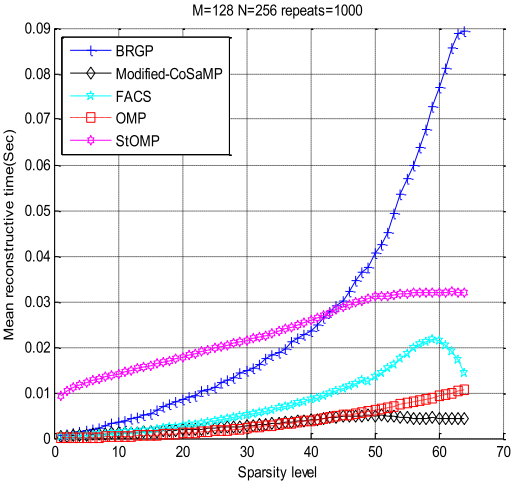

(b) Mean reconstructive time

Fig. 1. Comparison of reconstructive sparse signals in which the non-zero values obey the normal distribution.

Fig. 2(a) shows that the BRGP algorithm performs better than OMP, StOMP, Modified-CoSaMP and FACS on the frequency of exact reconstruction. From the results in Fig. 2-(a), we can see that the OMP, StOMP, Modified-CoSaMP and FACS algorithms can accurately reconstruct the signal at sparsity levels up to 28, 38, 42, and 52 respectively, while BRGP can accurately reconstruct the signal at a sparsity of 55. Fig. 2-(b) shows that the mean reconstruction time for BRGP, OMP, StOMP, Modified-CoSaMP and FACS algorithms at $1 \le K \le 64$. At $1 \le K \le 43$, the mean reconstructive time for BRGP is also only shorter than for StOMP, and then increases as the sparsity level increases.

Fig. 2(a) shows the advantages of the BRGP method of adding atoms, as in experiment 1. Because the coefficient ratio of the weighted 0–1 signal is greater than that for the Gaussian random signal, the BRGP gets a support set that is much faster and better and retains good performance to a higher sparsity level than in experiment 1. The trend of the time curve is similar with experiment 1, but the characteristics of the signals determine that the iterative number of the weighted 0–1 signal is smaller than the signal that the non-zero values obey $N(0, 1)$. The computational complexity of an algorithm equals the complexity of one iteration multiplied by

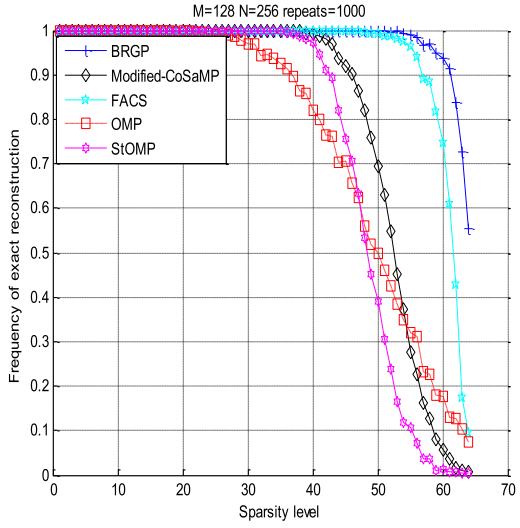

(a) Frequency of exact reconstruction

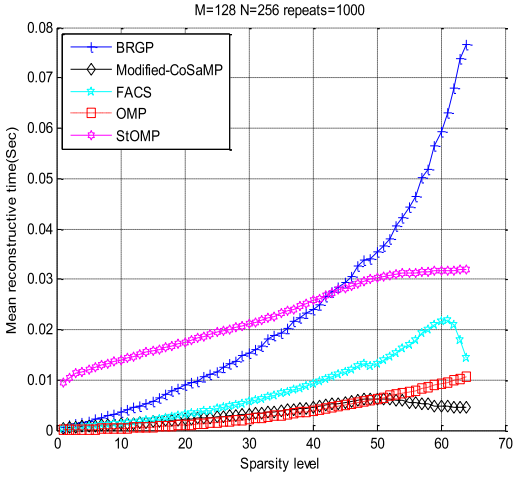

(b) Mean reconstructive time

Fig. 2. Comparison of indirect reconstructive weighted 0–1 sparse signal.

the number of iterations, so the mean reconstructive time of this experiment is a little less than in experiment 1.

5.3. Performance measures

We use a new performance measurement defined below to evaluate the proposed algorithm, called Average Support Cardinality Error (ASCE). The quality of the estimate of the sparse signal depends on the quality of the estimated support-set. Therefore, we use it to evaluate the quality of the supports-sets estimated by the sparse reconstruction algorithms, which is defined as

$$ASCE \triangleq 1 - \frac{1}{K}\mathbb{Z}|\tau \cap \hat{\tau}|, \tag{18}$$

where τ and $\hat{\tau}$ denote the actual and estimated support-sets, respectively.

To measure the level of under-sampling in CS, let us define the fraction of measurements $\alpha = M/N$.

In CS, we are mainly interested in the reconstruction performance for small values of α. Hence, we analyze the performance curves in this highly under-sampled region. The main steps involved in the simulation are the following:

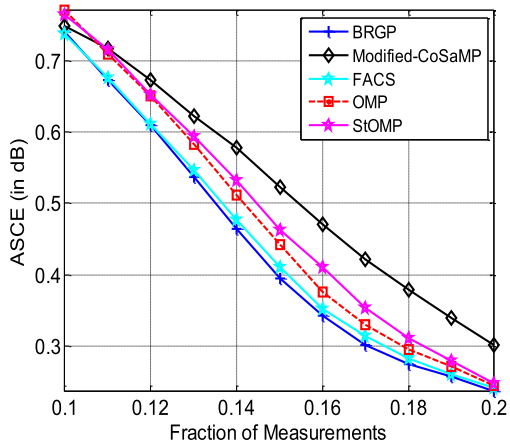

(a) ASCE vs. Fraction of measurements at 15db

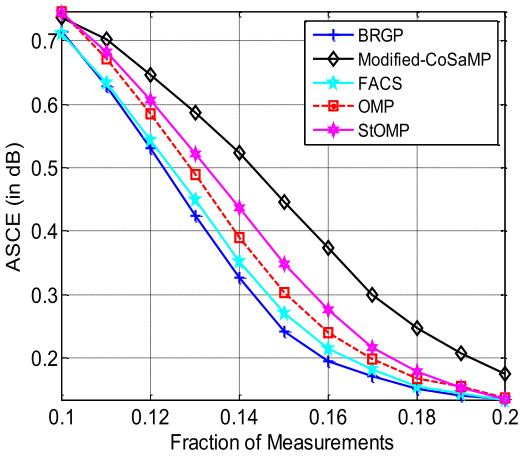

(b) ASCE vs. Fraction of measurements at 20db

Fig. 3. ASCE performance of these algorithms for Gaussian sparse signals with noise measurements (Signal to Measurement-Noise Ratio (SMNR) = 15 or 20 dB) (N = 500, K = 20).

(1) Fix K, $N = 500$ and choose an α so that the number of measurements M is an integer.
(2) Generate elements of $\Phi_{M\times N}$ independently from $N(0, 1/M)$ and normalize each column to unity.
(3) x is the same as that in experiment 5.1.
(4) For a noisy regime, the additive noise w is a Gaussian random vector whose elements are independently chosen from $N(0, \sigma_w^2)$.
(5) The measurement vector $b = \Phi x + w$.
(6) Apply the reconstruction methods independently.
(7) Repeat steps 3–6 $T = 100$ times. T indicates the number of times x is independently generated, for a fixed Φ.
(8) Repeat steps 2–7 $S = 20$ times. S indicates the number of times Φ is independently generated.

From Fig. 3, we can see that the ASCE performance of these algorithms decreases as the fraction of measurements increases from 0.1 to 0.2. Here BRGP performs better than the other algorithms in terms of ASCE for Gaussian sparse signals with noise measurements (Signal to Measurement-Noise Ratio (SMNR) = 15 or 20 dB). The ASCE of the BRGP algorithm is lower by 0.09, 0.01, 0.04, and 0.03 than the Modified-CoSaMP, FACS, StOMP and OMP algorithms, respectively, when SMNR = 15 dB. The ASCE of the BRGP algorithm is 0.12, 0.01, 0.06, 0.04 lower than that for the Modified-CoSaMP, FACS, StOMP and OMP algorithms, respectively, when SMNR = 20 dB.

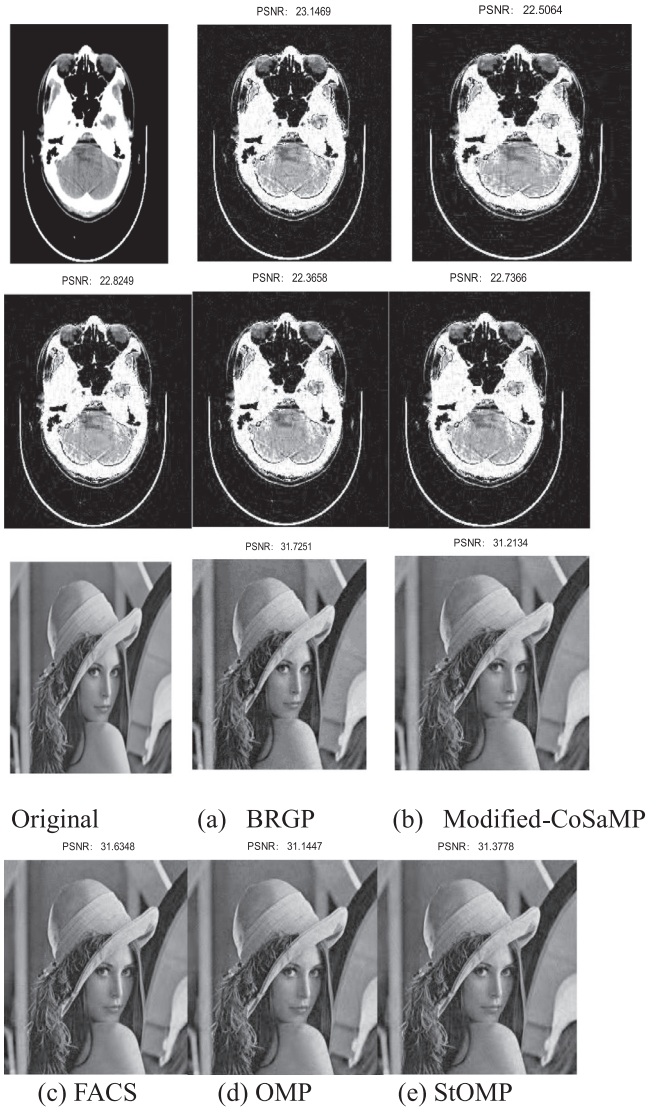

Fig. 4. The results of reconstructed 256×256 CT and Lena images from M/N = 50% sampling rate, PSNR in dB.

Because back-off and rectification in the BRGP method avoids the inclusion of incorrect atoms and rectifies the candidate support set, it makes the candidate support set approximate the target support set as closely as possible, while the other algorithms cannot guarantee obtaining correct atoms in the case of noisy measurements.

5.4. Image reconstructions by different methods

In this experiment set, we compare the performance of the BRGP, StOMP, OMP, modified-CoSaMP and FACS algorithms in a practical large-scale compressed imaging scenario. Two 256×256 test images of Computed Tomography (CT) and Lena are chosen and the sparsity matrix used was the popular Daubechies 9/7 wavelet. In order to obtain better experimental results, we use a Hadamard matrix measurement. Fig. 4 shows the PSNR of different algorithms reconstructing the original 256×256 images under the same conditions. We choose the CT image to test the sampling rate and PSNR of the experimental diagram, and Fig. 5 shows that the PSNR of the different algorithms increases with increasing sampling rate, but the PSNR of the BRGP algorithm is higher than for the other algorithms at the same sampling rate, in the range from

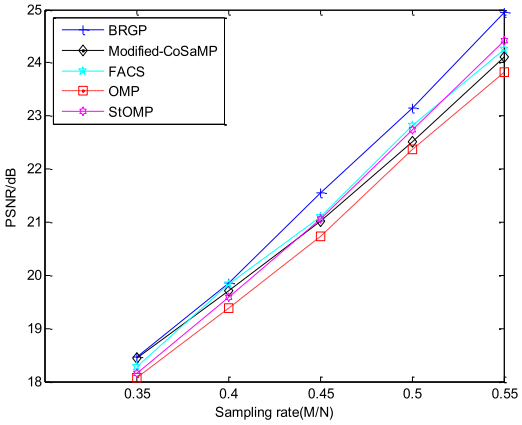

Fig. 5. Comparison of PSNR for the different algorithms at different sampling rates of the CT image.

0.35 to 0.55. The PSNR of the BRGP algorithm was higher by 0.434, 0.335, 0.720 and 0.404 than those of the Modified-CoSaMP, FACS, StOMP and OMP algorithms, respectively.

From the experimental analysis above, the back-off and rectification mechanism guarantees that the support set of the BRGP is better than the support set of the other algorithms, which also applies to the reconstruction of a two-dimensional signal. The BRGP approximates the original signal x better than the other comparison algorithms, and the mean square error $xerr = \frac{1}{m \times n} \sum_{i=1}^{m} \sum_{j}^{n} |x(i,j) - x'(i,j)|^2$ is smaller than for the other algorithms. Hence, the *PSNR* is larger with BRGP than with the other algorithms.

6. Conclusions

In this paper, the greedy pursuit algorithm, called back-off and rectification of greedy pursuit (BRGP), is proposed and analyzed for reconstruction applications in compressed sensing. As its name suggests, this reconstruction algorithm features a back-off and rectification mechanism to obtain a better support set, and includes the process of determining whether to back-off and update the support set to rectify an already obtained candidate support set. The underlying intuition of the BRGP, similar to that of other greedy pursuit algorithms, is to iteratively estimate the true support set. Extensive experimental results confirm that the BRGP algorithm can reconstruct a one-dimension signal or two-dimension image quickly and effectively.

Acknowledgments

This work was supported by the National Natural Science Foundation of China under Grants (No. 61602398, No. 61672447, No. 61711540306); Natural Science Foundation of Hunan Province, China (No. 2017JJ3316); The Research Foundation of Hunan Provincial Educational Department, China (No. 16C1547, No. 15C1330).

References

[1] X. Chen, M. Ma, A. Liu, Dynamic power management and adaptive packet size selection for IoT in e-Healthcare, Comput. Electr. Eng. (2017), doi:10.1016/j.compeleceng.2017.06.010.
[2] X. Liu, A. Liu, Z. Li, S. Tian, Y. Choi, H. Sekiya, J. Li, Distributed cooperative communication nodes control and optimization reliability for resource-constrained WSNs, Neurocomputing (2016). https://doi.org/10.1016/j.neucom.2016.12.105.
[3] X. Liu, G. Li, S. Zhang, A. Liu, Big program code dissemination scheme for emergency software-define wireless sensor networks, Peer Peer Netw. Appl. 3-4 (2017) 1–22 2017, doi:10.1007/s12083-017-0565-5.

[4] X. Liu, A. Liu, Q. Deng, H. Liu, Large-scale programing code dissemination for software defined wireless networks, Comput. J. (2018), doi:10.1093/comjnl/bxx014.
[5] J. Wang, A. Liu, S. Zhang, Key parameters decision for cloud computing: insights from a multiple game model, Concurrency Comput. (2017), doi:10.1002/cpe.4200.
[6] J. Wang, A. Liu, T. Yan, Z. Zeng, A resource allocation model based on double-sided combinational auctions for transparent computing, Peer Peer Netw. Appl. 10 (2017) 1–18 2017, doi:10.1007/s12083-017-0556-6.
[7] Y. Liu, A. Liu, S. Guo, Z. Li, Y. Choi, H. Sekiy, Context-aware collect data with energy efficient in cyber-physical cloud systems, Fut. Gen. Comput. Syst. (2017), doi:10.1016/j.future.2017.05.029.
[8] S. Wang, C. Deng, W. Lin, G.-B. Huang, B. Zhao, NMF-based image quality assessment using extreme learning machine, IEEE Trans. Cybern. 47 (1) (2017) 232–243.
[9] C. Liu, L. He, Z. Li, J. Li, Feature driven active learning for hyperspectral image classification, IEEE Trans. Geosci. Remote Sens. 56 (1) (2018) 341–354, doi:10.1109/TGRS.2017.2747862.
[10] C. Luo, Z. Li, K. Huang, J. Feng, M. Wang, Zero-Shot learning via attribute regression and class prototype rectification, IEEE Trans. Image Process. 27 (2) (2018) 637–648, doi:10.1109/TIP.2017.2745109.
[11] Y. Cen, R. Zhao, L. Cen, L. Cui, Z. Miao, Z. Wei, Defect inspection for TFT-LCD images based on the low-rank matrix reconstruction, Neurocomputing 149 (3) (2015) 1206–1215.
[12] H. Wang, Y. Cen, Z. He, R. Zhao, Y. Cen, F. Zhang, Robust generalized low-rank decomposition of multi-matrices for image recovery, IEEE Trans. Multimedia 9 (5) (2017) 969–983.
[13] S. Tian, X. Fan, Z. Li, T. Pan, Y. Choi, H. Sekiya, Orthogonal-gradient measurement matrix construction algorithm, Chin. J. Electron. 25 (CJE-1) (2016) 81–87.
[14] Y. Zheng, B. Jeon, L. Sun, J. Zhang, H. Zhang, Students t-Hidden Markov Model for unsupervised learning using localized feature selection, IEEE Trans. Circuits Syst. Video Technol. (2017), doi:10.1109/TCSVT.2017.2724940.
[15] Q. Liu, A. Liu, On the hybrid using of unicast-broadcast in wireless sensor networks, Comput. Electr. Eng. (2018). http://dx.doi.org/10.1016/j.compeleceng.2017.03.004.
[16] Y. Liu, A. Liu, Y. Li, Z. Li, Y. Choi, H. Sekiya, J. Li, APMD: a fast data transmission protocol with reliability guarantee for pervasive sensing data communication, Perv. Mobile Comput. (2017), doi:10.1016/j.pmcj.2017.03.012.
[17] E.J. Candès, T. Tao, Decoding by linear programming, IEEE Trans. Inf. Theory 51 (12) (2005) 4203–4215.
[18] D.L. Donoho, Compressed sensing, IEEE Trans. Inf. Theory 52 (4) (2006) 1289–1306.
[19] Z. Li, J. Xie, D. Tu, Y. Choi, Sparse signal recovery by stepwise subspace pursuit in compressed sensing, Int. J. Distrib. Sens. Netw. 9 (8) (2013) 798537.
[20] J. Fang, L. Zhang, H. Li, Two-dimensional pattern-coupled sparse Bayesian learning via generalized approximate message passing, IEEE Trans. Image Process. 25 (6) (2016) 2920–2930.
[21] H. Duan, L. Zhang, J. Fang, L. Huang, H. Li, Pattern-coupled sparse Bayesian learning for inverse synthetic aperture imaging, IEEE Signal Process. Lett. 22 (11) (2015) 1995–1999.
[22] Z. Li, J. Xie, G. Zhu, X. Peng, Y. Choi, R. Xie, Block-based projection matrix design for compressed sensing, Chin. J. Electron. 25 (3) (2016) 551–555.
[23] Y. Li, W. Dai, J. Zou, H. Xiong, Y.F. Zheng, Structured sparse representation with union of data-driven linear and multilinear subspaces model for compressive video sampling, IEEE Trans. Signal Process. 65 (19) (2017) 5062–5077.
[24] E.J. Candès, J. Romberg, T. Tao, Robust uncertainty principles: exact signal reconstruction from highly incomplete frequency information, IEEE Trans. Inf. Theory 52 (2) (2006) 489–509.
[25] E. Liu, V.N. Temlyakov, The orthogonal super greedy algorithm and applications in compressed sensing, IEEE Trans. Inf. Theory 58 (4) (2012) 2040–2047.
[26] J.A. Tropp, A.C. Gilbert, Signal recovery from random measurements via orthogonal matching pursuit, IEEE Trans. Inf. Theory 53 (12) (2007) 4655–4666.
[27] A.C. Gilbert, S. Guha, P. Indyk, et al., Near-optimal sparse Fourier representations via sampling, in: Proceedings of the Thiry-fourth Annual ACM Symposium on Theory of Computing, ACM, 2002, pp. 152–161.
[28] A.C. Gilbert, M. Strauss, Improved time bounds for near-optimal sparse fourier representations. Optics & Photonics, Int. Soc. Opt. Photon. 5914 (2005) (2005) 398–412.
[29] A.C. Gilbert, M.J. Strauss, J.A. Tropp, R. Vershynin, Algorithmic linear dimension reduction in the l_1 norm for sparse vectors, in: Proceedings of the 44th Deanna Needell, 2006.
[30] A.C. Gilbert, M.J. Strauss, J.A. Tropp, R, et al., One sketch for all: fast algorithms for compressed sensing, in: Proceedings of the Thirty-Ninth Annual ACM Symposium on Theory of Computing, 13, ACM, 2007, pp. 237–246.
[31] D. Needell, J. Tropp, R. Vershynin, Greedy signal recovery review, in: IEEE 42nd Asilomar Conference on Signals, Systems and Computers, 2008, pp. 1048–1050.
[32] S.S. Chen, D.L. Donoho, M.A. Saunders, Atomic decomposition by basis pursuit, SIAM J. Sci. Comput. 20 (1) (1998) 33–61.
[33] J.A. Tropp, A.C. Gilbert, Signal recovery from random measurements via orthogonal matching pursuit, IEEE Trans. Inf. Theory 53 (12) (2007) 4655–4666.
[34] S. Chatterjee, D. Sundman, M. Skoglund, Look ahead orthogonal matching pursuit, in: 2011 IEEE International Conference on Acoustics, Speech and Signal Processing (ICASSP), IEEE, 2011, pp. 4024–4027.
[35] S. Kwon, J. Wang, B. Shim, Multipath matching pursuit, IEEE Trans. Inf. Theory 60 (5) (2014) 2986–3001.
[36] D.L. Donoho, Y. Tsaig, I. Drori, et al., Sparse solution of underdetermined systems of linear equations by stagewise orthogonal matching pursuit, IEEE Trans. Inf. Theory 58 (2) (2012) 1094–1121.
[37] W. Dai, O. Milenkovic, Subspace pursuit for compressive sensing signal reconstruction, IEEE Trans. Inf. Theory 55 (5) (2009) 2230–2249.
[38] D. Needell, J.A. Tropp, CoSaMP: Iterative signal recovery from incomplete and inaccurate samples, Appl. Comput. Harmon. Anal. 26 (3) (2009) 301–321.
[39] S.K. Ambat, S. Chatterjee, K.V.S. Hari, On selection of search space dimension in compressive sampling matching pursuit, TENCON 2012-2012 IEEE Region 10 Conference, IEEE, 2012.
[40] W. Wang, L. Ni, Multipath subspace pursuit for compressive sensing signal reconstruction, in: 2014 7th International Congress on Image and Signal Processing (CISP), IEEE, 2014, pp. 1141–1145.
[41] S.K. Ambat, S. Chatterjee, K.V.S. Hari, Fusion of algorithms for compressed sensing, IEEE Trans. Signal Process. 61 (14) (2013) 3699–3704.
[42] S. Pudlewski, A. Prasanna, T. Melodia, Compressed-sensing-enabled video streaming for wireless multimedia sensor networks, IEEE Trans. Mob. Comput. 11 (6) (2012) 1060–1072.